buildings

MDPI

Article

Impact of Aging and Low Temperatures on the Mechanical Properties of Low-Cost Seismic Isolator Prototypes

Isabel C. Velasco-Cuervo [1,*], Erika D. Lemos-Micolta [1], Ingrid E. Madera-Sierra [2], Manuel Alejandro Rojas-Manzano [1], Mario F. Muñoz-Velez [3], Orlando Cundumí [1], Edwin Patino [4], Manuel Salmeron-Becerra [4], Shirley J. Dyke [4,5] and Mirian Velay-Lizancos [4]

[1] Departamento de Ingeniería Civil e Industrial, Pontificia Universidad Javeriana Cali, Calle 18 #118-200, Santiago de Cali 760031, Colombia; erikalemos08@javerianacali.edu.co (E.D.L.-M.); alejandro.rojas@javerianacali.edu.co (M.A.R.-M.); orlando.cundumi@javerianacali.edu.co (O.C.)
[2] Departamento de Tecnología de la Construcción, Escuela de Arquitectura, Facultad de Artes Integradas, Universidad del Valle, Calle 13 #100-00, Santiago de Cali 760032, Colombia; ingrid.madera@correounivalle.edu.co
[3] Grupo de Materiales Compuestos (GMC), Escuela de Ingenieria de Materiales, Universidad del Valle, Calle 13 #100-00, Santiago de Cali 760034, Colombia; mario.fernando.munoz@correounivalle.edu.co
[4] Lyles School of Civil and Construction Engineering, Purdue University, 585 Purdue Mall, West Lafayette, IN 47907-2088, USA; patino7@purdue.edu (E.P.); salmeron@purdue.edu (M.S.-B.); sdyke@purdue.edu (S.J.D.); mvelayli@purdue.edu (M.V.-L.)
[5] School of Mechanical Engineering, Purdue University, 585 Purdue Mall, West Lafayette, IN 47907-2088, USA
* Correspondence: isabelvelascoc@javerianacali.edu.co

Abstract

Seismic isolation systems are an effective passive protection strategy that decouples structures from ground motion. Their performance depends heavily on the elastomeric materials used, which must retain mechanical integrity under environmental stressors. In recent years, low-cost isolators made from natural and recycled rubber have gained attention as an affordable solution for protecting low-rise buildings in seismic-prone developing regions, particularly due to their environmental benefits and ease of installation. However, their long-term performance under real environmental conditions remains insufficiently explored. This study evaluates the durability of two types of low-cost seismic isolators: those made with natural rubber matrices (UN-FREIs) and those that use recycled rubber matrices (UR-FREIs). Mechanical tests were carried out before and after exposing the specimens to accelerated aging and low-temperature conditions, simulating environmental degradation. Changes in stiffness, damping, and energy dissipation were analyzed for both the rubber matrix and the scaled isolator prototypes. The findings indicate that both materials degrade over time, with recycled rubber exhibiting greater susceptibility to stiffness loss at low temperatures. Nevertheless, both isolator types maintained functional performance after aging, supporting their applicability in regions with moderate thermal variations. These results provide evidence for the feasibility of adopting low-cost isolators in low-rise buildings exposed to variable climates, while also emphasizing the need for standardized durability protocols during the design stage.

Keywords: low-cost seismic isolators; natural and recycled rubber; durability; aging test; low temperatures

check for updates

Academic Editor: Muxuan Tao

Received: 7 May 2025
Revised: 31 May 2025
Accepted: 9 June 2025
Published: 26 June 2025

Citation: Velasco-Cuervo, I.C.; Lemos-Micolta, E.D.; Madera-Sierra, I.E.; Rojas-Manzano, M.A.; Muñoz-Velez, M.F.; Cundumí, O.; Patino, E.; Salmeron-Becerra, M.; Dyke, S.J.; Velay-Lizancos, M. Impact of Aging and Low Temperatures on the Mechanical Properties of Low-Cost Seismic Isolator Prototypes. *Buildings* **2025**, *15*, 2238. https://doi.org/10.3390/buildings15132238

Copyright: © 2025 by the authors. Licensee MDPI, Basel, Switzerland. This article is an open access article distributed under the terms and conditions of the Creative Commons Attribution (CC BY) license (https://creativecommons.org/licenses/by/4.0/).

1. Introduction

Seismic risk varies depending on the hazard zone and the structural vulnerability of inhabited buildings. Since the hazard zone is immutable, various seismic control systems

have been developed to mitigate this risk, including base isolation systems [1–3]. These systems reduce structural vulnerability [4–6] by employing passive protection mechanisms that decouple the structure from ground motion through devices that operate without additional energy. Seismic isolators absorb earthquake-induced deformations, preventing damage to both structural and non-structural components. Currently, base isolation systems commonly utilize steel-reinforced isolators (SRIs), which are widely adopted in many countries. However, their high manufacturing and validation costs have limited their application in developing nations [7,8].

To address this limitation, researchers have developed low-cost seismic isolation devices that are more affordable due to design and construction optimizations. These include the use of fiber reinforcement, which reduces weight, and design modifications that simplify installation. Referred to as low-cost seismic isolators by Madera-Sierra [9] and Ortega [10], these devices have been developed using both natural rubber matrices (UN-FREIs) and recycled tire rubber matrices (UR-FREIs), and their mechanical properties and characteristics have been confirmed through reduced- and real-scale prototypes [11–15].

In this context, Meza-Muñoz et al. [16] developed a matrix for seismic isolators using recycled rubber from vehicle tires, aiming to provide an environmentally friendly and cost-effective alternative to traditional materials. Their research demonstrated the potential of this matrix in terms of its mechanical performance and sustainability. Building upon this, Rivas-Ordonez et al. [17] evaluated different alternatives to enhance the mechanical properties of seismic isolators made from recycled rubber. Their study provided valuable insights into optimizing formulation strategies to improve stiffness and energy dissipation, further supporting the viability of such devices in low-income seismic regions.

This approach not only reduces production costs but also contributes to environmental protection by reusing discarded tires. Low-cost seismic isolators offer protection for low-rise structures, which constitute the majority of residential buildings in developing countries. Consequently, they present a practical solution for safeguarding millions of lives without compromising structural safety or functionality. However, before mass production and implementation can proceed, it is essential to evaluate the durability of these isolators under varying temperature conditions and aging processes. These factors can affect the performance of the polymers used in the isolators, potentially leading to changes in device behavior over time.

Lemos-Micolta et al. [18] conducted a comprehensive investigation on how various environmental agents—including humidity, ultraviolet (UV) radiation, and temperature fluctuations—can significantly impact both the rubber matrix and reduced-scale prototypes of seismic isolators. Their findings highlighted material degradation processes that alter the stiffness, energy dissipation, and elastic recovery of the devices over time, particularly in recycled rubber systems. This underscores the importance of assessing long-term performance in environments subject to thermal and oxidative stress. Similarly, studies conducted by Calabrese et al. [19] and Toopchi-Nezhad et al. [20] emphasized the necessity of incorporating durability assessments into the design and validation stages of seismic isolation systems. These authors pointed out that, while mechanical efficiency is often prioritized in early development, the lack of long-term performance evaluations can compromise the reliability and safety of the devices in service. Calabrese et al., for instance, proposed durability testing protocols that simulate real-world conditions, while Toopchi et al. argued for the standardization of environmental exposure methods in seismic isolator research. Moreover, other researchers have also addressed the critical influence of environmental aging on rubber-based materials, such as ozone cracking, moisture absorption, and glass transition phenomena at low temperatures. It has also been established that thermal and environmental aging can degrade both the microstructural integrity and macroscopic

mechanical performance of seismic isolators. Specifically, it causes a degradation of the crosslinking network, which leads to decreased elongation at break, increasing stiffness and embrittlement. This reduces their elastic recovery and the isolators' ability to absorb and dissipate seismic energy [19–22]. These converging insights underscore the global relevance of investigating durability in low-cost isolators to ensure both structural resilience and long-term sustainability, especially in regions exposed to harsh or variable climates.

Against this research backdrop, this study focuses on evaluating the durability of low-cost seismic isolators manufactured with natural rubber matrices (UN-FREIs) and recycled rubber matrices (UR-FREIs). The evaluation considers two key factors affecting the performance of the isolators and their constituent materials: (I) natural aging associated with service life, and (II) the influence of low temperatures. These factors are analyzed to assess the behavior of the devices in regions with significant seasonal variations, thereby broadening their global applicability. To achieve this, the behavior of both polymeric matrices and reduced-scale isolator prototypes is evaluated through mechanical testing conducted before and after accelerated aging and low-temperature exposure. The results of this research will help to identify the time and temperature conditions that affect the durability and performance of low-cost seismic isolators.

2. Materials and Methods

2.1. Materials

2.1.1. UR-FREI

For the construction of the matrix and small-scale prototypes of recycled rubber seismic isolators, a detailed procedure was followed. This included material preparation, specimen shaping, and prototype fabrication using hot pressing.

Material Preparation

This procedure was carried out at Occidental de Cauchos. The rubber used in this study came from the shredding of Bridgestone truck tires, following the recommendations established by Ortega [10]. The raw material was shredded and then screened to obtain a mixture with a controlled particle size distribution. Two types of granulometry were selected—fine and medium—which were combined to achieve an adequate composition in terms of compaction and adhesion with the binder.

Construction of Specimens

For the construction of the specimens, a mixture of crushed rubber and polyurethane binder was prepared in a 1:4 ratio. This mixture was poured into molds preheated to 140 °C for 10 min to ensure the homogeneous distribution of the material. The molds were then subjected to a pressing process at a speed of 5 mm/s and a temperature of 140 °C for 4 min. This procedure produced specimens with a compact and uniform structure, suitable for subsequent characterization and analysis.

Fabrication of Small-Scale Prototypes

In the final stage, small-scale prototypes were fabricated using a hydraulic press at Pontificia Universidad Javeriana Cali (PUJ Cali) and a modular mold specifically designed for this purpose. The process involved alternating 15 layers of the rubber–binder mixture with 14 layers of polyester fiber, following the structural design of the seismic isolators. During assembly, the modular mold was progressively built as each layer was added, ensuring the proper alignment of the materials. Finally, the structure was pressed at 140 °C for 20 min to achieve material consolidation and optimal adhesion between the rubber and fiber reinforcement layers.

This procedure enabled the production of specimens and small-scale seismic isolator prototypes with adequate mechanical properties for subsequent evaluation and experimental validation.

2.1.2. UN-FREI

For the manufacture of specimens and prototypes using a natural rubber matrix, a rigorous procedure was followed. This included the preparation of the base mixture, sheet pressing, and final prototype construction through controlled thermal processes.

Natural Rubber Matrix Preparation

This procedure was carried out at Surtidor Industrial S.A. Following the recommendations of Madera [9], the natural rubber matrix was formulated by combining 11 components in specific proportions. During the mixing process, time and temperature were strictly controlled to ensure a homogeneous and stable composition. This process resulted in a uniform raw material suitable for the manufacture of both specimens and prototypes.

Specimen Construction

Once the 2 mm thick rubber sheets were obtained, 75 mm circles were cut and bonded to fiber circles of the same diameter. The assembled specimens were then placed into molds designed for subsequent forming. They were subjected to a pressing process at 100 °C for 15 min to ensure the proper compaction and adhesion of the materials. This step was essential for achieving structures with uniform dimensions and consistent mechanical properties.

Manufacture of Small-Scale Prototypes

For the construction of the prototypes, 15 rubber sheets for each unit were pre-pressed at a temperature of 70 °C for 2 min each. After completing this process, the final prototypes were assembled by incorporating a covering sheet that wrapped the entire surface of the cylinder. Finally, the prototypes were subjected to thermal exposure at 201 °C for 1 h, allowing for final material consolidation and resulting in a structure with the properties required for subsequent analysis and validation.

This procedure enabled the production of specimens and prototypes with physical and mechanical properties suitable for experimental studies in structural and seismic isolation applications.

2.2. Fabrication of the Seismic Isolator Prototypes

The prototypes were manufactured using the same natural and recycled rubber matrices described in Section 2.1 of this article. The small-scale prototypes were developed based on the tests conducted by Lossano et al. [12–14,23], for both recycled and natural rubber matrices. To determine the appropriate scale for the prototypes, an analysis was carried out using seven seismic records representative of regions in Italy. The structural model used for this analysis consisted of a structure supported by four columns, each bearing a load of 19.25 kN. The target design period for the base-isolated structure was 1.16 s. The final dimensions obtained for the prototypes are presented in Figure 1 [23]. To guarantee that the reduced-scale prototypes provide meaningful insights into the behavior of full-scale isolators, dynamic equivalence through geometric scaling laws were applied, ensuring that the height-to-diameter ratios of the reduced-scale prototypes closely match those of full-scale devices. This helped to maintain a similar distribution of shear and compressive stresses, which are critical in seismic isolation systems [14].

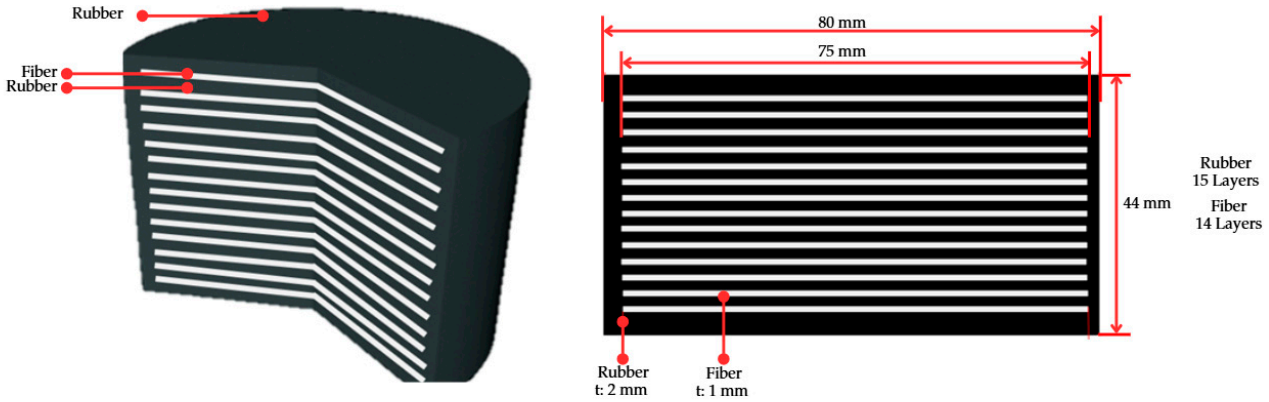


Figure 1. Dimensions of the UN-FREI and UR-FREI small-scale prototypes.

2.3. Pre-Conditioning of Specimens and Small-Scale Prototypes

2.3.1. Low-Temperature Exposure

This procedure was carried out through three cycles of immersion in a mixture of 95% isopropyl alcohol and dry ice, with each cycle consisting of one minute of immersion. Controlled temperatures of −40 °C were reached (Figure 2a), in accordance with ASTM D746-20 [24] and the recommendations of Toopchi-Nezhad et al. [20].



(**a**) (**b**)

Figure 2. Pre-conditioning of specimens and small-scale prototypes. (**a**) Low-temperature exposure and (**b**) accelerated aging.

2.3.2. Accelerated Aging

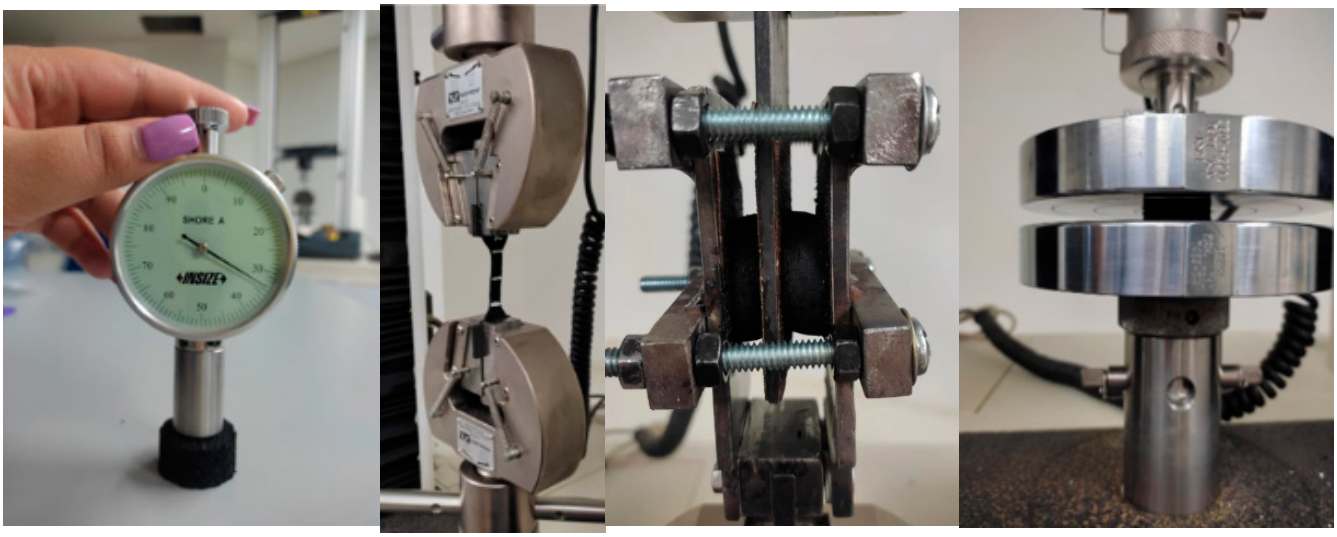
The specimens (both matrix and isolator prototypes) were subjected to an accelerated aging process based on the recommendations of the Italian standard [19]. This involved exposure to 100 °C in an air oven for six weeks (Figure 2b), which corresponds to 28 years of natural aging, according to AASHTO M251-06 [8].

2.4. Mechanical Characterization of Specimens

In all the tests described in this section, three (3) specimens were used for each experimental condition, including both types of materials (UN-FREIs and UR-FREIs). For the low-temperature exposure tests, 3 specimens per material were tested and for the accelerated aging evaluation, and 3 specimens per material were tested for each week of exposure. Each specimen was tested only once and discarded afterward to avoid cumulative effects. All specimens were manufactured following standardized procedures to ensure consistency in geometry, vulcanization, and material composition.

2.4.1. Hardness

Hardness was measured using a Shore A hardness tester (Figure 3a), in accordance with ASTM D2240-05 [25]. The specimens had a diameter of 28.6 mm and a height of 12.5 mm. Three specimens were tested, and five hardness readings were taken on each one.



(**a**) (**b**) (**c**) (**d**)

Figure 3. Specimens for: (**a**) hardness, (**b**) tension, (**c**) shear modulus, and (**d**) monotonic compression.

2.4.2. Tensile Properties

The tensile mechanical properties of the matrices were evaluated in accordance with ASTM D412-06 (Procedure A) [26]. The specimens had a reduced cross-section with a length of 33 mm, a width of 6 mm, and a thickness of 3 mm. The load was applied at a speed of 500 mm/min for the UN-FREI specimens and 50 mm/min for the UR-FREI specimens. In the case of the recycled rubber, a lower speed allowed for greater elongation before failure. The tests were performed using an Instron universal testing machine at the PUJ Cali laboratory, equipped with a 10 kN load cell (Figure 3b).

2.4.3. Shear Modulus

To simulate the dynamic stress characteristics of a low- to moderate-frequency seismic event, the behavior of the isolators was evaluated under cyclic shear loads, following the recommendations of Method B in ASTM D4014 [27]. The specimens had a diameter of 28.6 mm and a height of 12.5 mm. They were subjected to controlled cyclic deformations equivalent to 10%, 20%, 30%, 40%, 50%, 75%, 100%, and 150% of the specimen's initial height. Each cycle was applied over a period of 9 s using an Instron testing machine equipped with a 10 kN load cell (Figure 3c). Although the 9 s cycle period was determined by the capabilities of the testing equipment, previous studies on natural rubber have shown that this period does not significantly influence the results; therefore, the same parameters were applied to recycled rubber specimens to ensure data comparability. This test allowed for the analysis of the material's ability to dissipate energy and maintain stiffness under reversible cyclic loading [10].

2.4.4. Monotonic Compression

The monotonic compression test was performed in accordance with ASTM D575, Method A [28]. The specimens had a diameter of 28.6 mm and a height of 12.5 mm and were compressed to 80% of their initial height (equivalent to 12 mm) at a constant speed of 12 mm/min. The procedure was repeated over three cycles. Before these main cycles, a

preload cycle was applied up to 40% deformation (6 mm) to stabilize the material response and minimize the loss of initial stiffness (Figure 3d), a phenomenon commonly referred to as the Mullins effect (ASTM D575, 2018) [28]. This effect refers to the reduction in stiffness observed in elastomeric materials during the initial loading cycles.

2.5. Mechanical Characterization of Small-Scale Prototypes

To establish direct comparisons in the results, the seismic isolator prototypes were tested in their original state, without having been previously subjected to aging processes or low-temperature exposure. These devices were considered the control group. The tests performed are described below.

In addition, to ensure consistent and independent results across all test conditions, two small-scale prototypes were used for each material type (UN-FREIs and UR-FREIs) during the low-temperature test. Additionally, two new prototypes were tested for each exposure week in the accelerated aging test. No prototype was reused between different tests or exposure periods; each one was tested only once and subsequently discarded. The methodologies and procedures applied in each test are described in the following sections.

2.5.1. Shear Compression Test

A protocol developed to evaluate the mechanical performance of the seismic isolator [9] prototypes was used, applying six levels of deformation: 25%, 50%, 67%, 100%, 100%, and 75% of the maximum deformation of 29 mm (Figure 4a). The test was conducted at Purdue University's Intelligent Infrastructure Systems Laboratory (IISL).

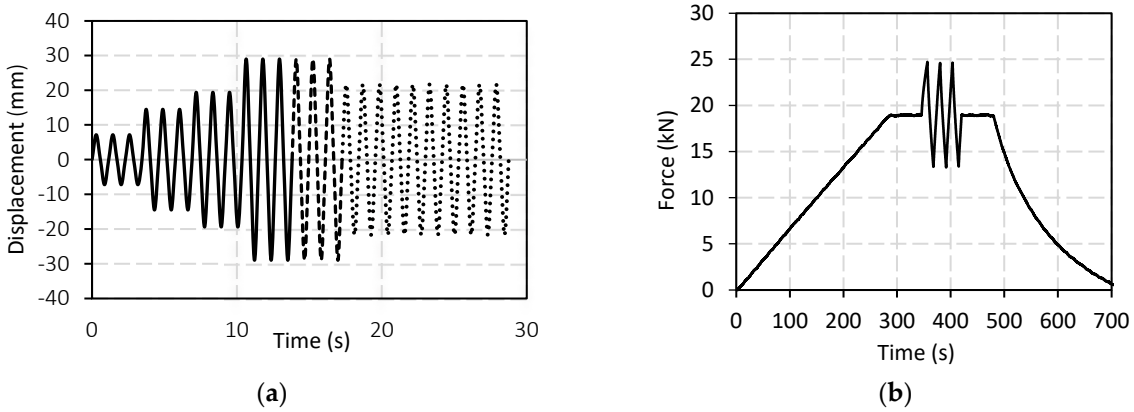


Figure 4. (**a**) Shear compression test protocol, (**b**) cyclic compression test protocol [18].

2.5.2. Cyclic Compression Test

A protocol designed to evaluate the mechanical response of seismic isolators [9] was used for this test, following a three-phase procedure to assess displacements under variable compression conditions. In the first phase, a progressive load was applied until the design load of 19 kN was reached. In the second phase, three loading and unloading cycles were performed up to ±30% of the design load. Finally, in the third phase, the device was completely unloaded at a constant speed (Figure 4b).

3. Results and Discussion

3.1. Mechanical Evaluation of Isolator Matrix

3.1.1. Hardness (H)

Specimens subjected to low temperatures (LT) showed a significant increase in the surface hardness of both polymeric matrices (UN-FREI and UR-FREI). The average values obtained for five samples in each condition are detailed below (Table 1).

Table 1. Hardness results for low temperatures.

	UR-FREI	UN-FREI
Initial Condition (Shore A)	72.4	53.4
After Exposition LT (Shore A)	79.6	62.2
Increase (%)	9.94	16.51

The increases of 9.94% in the hardness of the recycled rubber matrix (UR-FREI) and 16.51% in the natural rubber matrix (UN-FREI) are evidence of the sensitivity of both formulations to low temperatures (Table 1), which is more pronounced in the natural rubber. This behavior can be explained by the significant reduction in the segmental mobility of the polymeric chains when the temperature drops towards or below the glass transition temperature (Tg), which causes a general hardening of the material and a loss of its elastic deformation capacity [29]. For both matrices (UR-FREI and UN-FREI), the Shore A hardness readings for each specimen varied within ±2 units of the mean value across five measurements per specimen. This reflects the localized microstructural differences, particularly in UR-FREI specimens, which include recycled rubber particles of varying sizes and shapes.

Additionally, several studies have shown that some elastomers, such as natural rubber, can undergo crystallization processes at low temperatures. This thermal crystallization results in the formation of semi-crystalline regions, which increases the hardness and stiffness of the material [30,31]. This phenomenon is more evident in elastomers with regular molecular structures, since the alignment of the chains facilitates the nucleation and growth of crystals under cooling conditions.

Figure 5 shows the results obtained in the Shore A hardness evaluation for both matrices (UR-FREI and UN-FREI), where an increasing trend is observed during the accelerated aging process at 100 °C; this confirms the thermal susceptibility of these materials. The recycled rubber matrix (UR-FREI) shows a progressive increase in hardness from 72.4 to 83.1 Shore A units at the end of the sixth week of exposure, equivalent to an increase of 15%. In the case of natural rubber (UN-FREI), the increase was more moderate, going from 53.4 to 62.6 units, representing an increase of 17%.

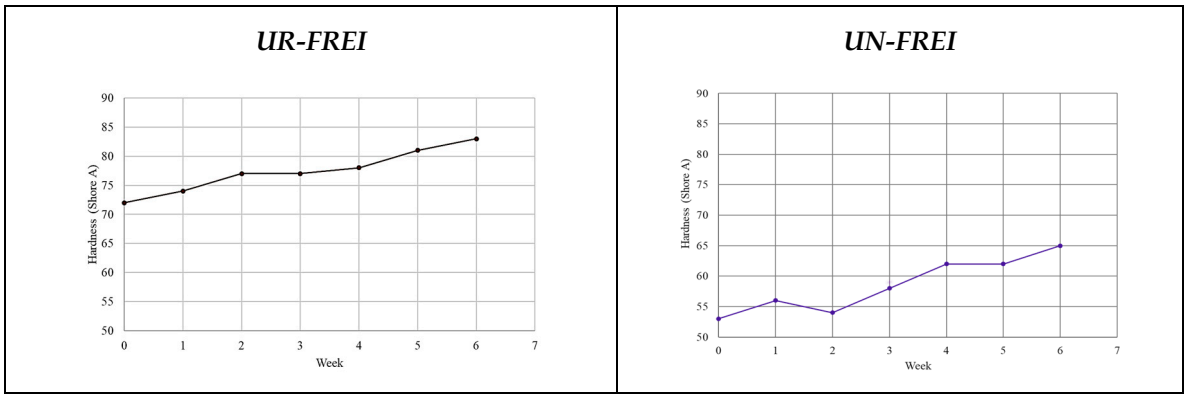


Figure 5. Hardness results for specimens subjected to accelerated aging.

The hardness behavior observed in the two materials can be associated with thermal aging processes that induce modifications in the crosslinking network of natural rubber. As reported by South et al. (2003), prolonged exposure to elevated temperatures generates a redistribution of sulfur bonds in the polymeric matrix, with a reduction in polysulfidic bonds, characterized by their flexibility, and an increase in disulfidic and monosulfidic

bonds, which are structurally stiffer [21]. This internal chemical transformation, a product of thermoinduced mechanisms, increases the stiffness of the material and reduces its deformation capacity.

In contrast, the greater increase in the hardness of the UR-FREI matrix could be attributed to the presence of carbon black and crosslinking residues in the recycled rubber, which could promote temperature hardening. Cossio Urán et al. (2011) reported similar effects, with increased hardness after aging due to additional bond formation in mixtures with high carbon black loading [32].

3.1.2. Maximum Tensile Strength and Elongation at Failure (T)

Exposure to low temperatures produced different effects on the mechanical properties of the UR-FREI and UN-FREI matrices (Figure 6). In the UR-FREI specimens, a marked decrease in peak stress (71%) and a moderate reduction in strain capacity (14%) were evident. This loss of performance can be attributed to the agglomerated nature of UR-FREI, the porosity of which favors the infiltration of the cryogenic medium, deteriorating its internal structure. In this study, the porosity of the UR-FREI and UN-FREI matrices was not directly measured; however, based on microstructural observations from previous research and the intrinsic differences in the studied fabrication methods and material compositions of these two matrices, it could be inferred that the UR-FREI matrix is more prone to porosity-related infiltration effects under exposure to low temperatures. In addition, the binder that binds the particles together could undergo crystallization at low temperatures, which increases the stiffness and brittleness of the system. The maximum tensile strength exhibited a variability of approximately ±8% between specimens for the UR-FREI matrix and ±5% for the UN-FREI matrix under reference (unaged) conditions. After exposure to low temperatures and accelerated aging, the variability slightly increased to ±10% for UR-FREI and ±6% for UN-FREI, consistent with the increased material heterogeneity after degradation.

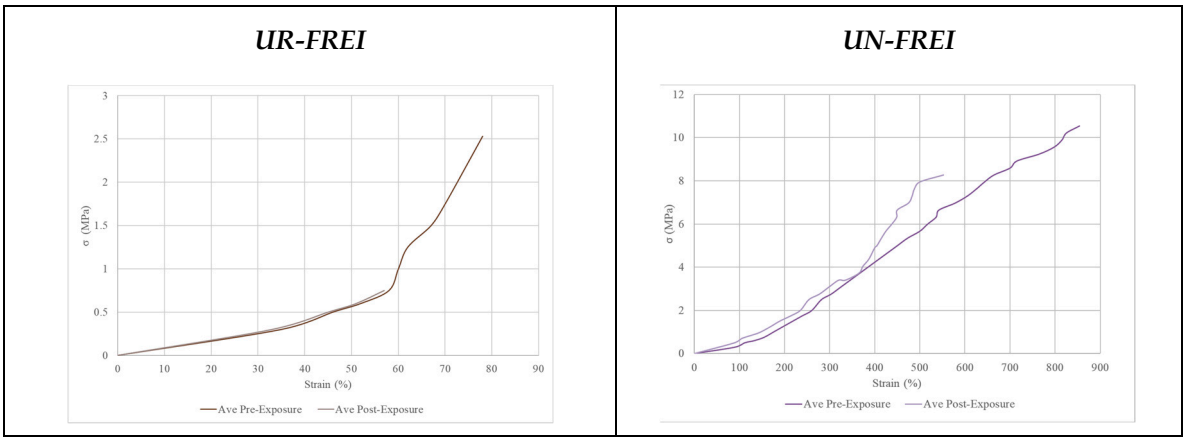


Figure 6. Results of stress exposure to low temperatures.

In contrast, while the UN-FREI matrix also showed deterioration, it exhibited greater mechanical stability. The 21% reduction in maximum strength and 32% reduction in elongation can be explained by cold-induced crystallization processes, characteristic of natural rubber. According to other researchers, in sustained cold environments (−25 °C), vulcanized elastomers suffer progressive loss of strength, elongation, and elasticity, accompanied by surface hardening due to the generation of new crosslinks and the possible crystallization of polymer chains [1,2,22].

Alternatively, Kabakçi et al. (2022) [33] point out that composites with recycled rubber present a stiffer matrix and lower deformation capacity than virgin rubber, especially under severe conditions, which would explain the inferior performance of UR-FREI compared to UN-FREI. These differences should be considered in structural applications subjected to thermal cycling, where the energy absorption capacity and ductility of the material are fundamental.

However, the results obtained on polymeric matrices after exposure to accelerated thermal aging at 100 °C for six weeks (Figure 7) show a progressive degradation over time in terms of mechanical properties. For the UR-FREI matrix, a 96% reduction in the strain at break and a 45% reduction in the ultimate strength were evidenced. For the UN-FREI matrix, the loss was even more pronounced in terms of elongation (97%) and 65% in maximum stress. From week three onwards, both materials showed severe brittleness, to the point of fracture during test set-up.

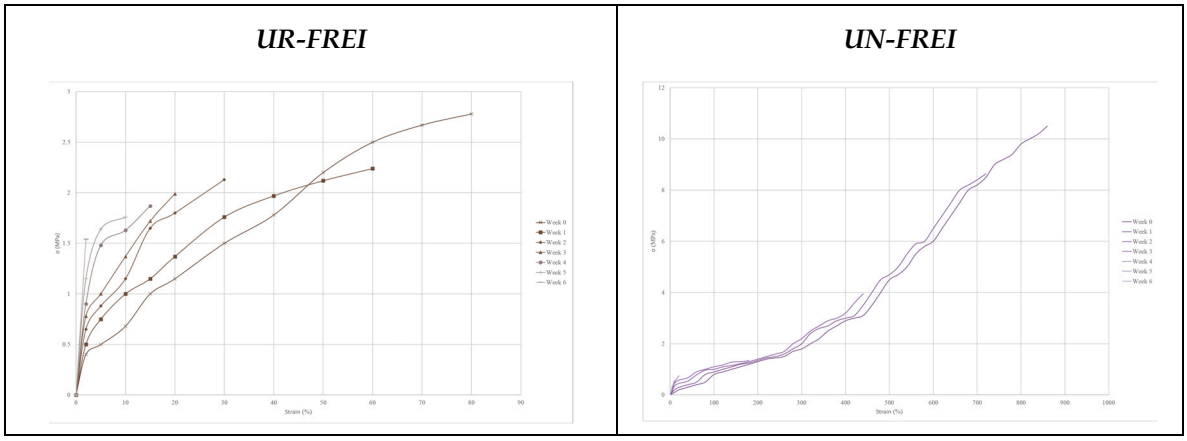


Figure 7. Accelerated aging stress results.

This behavior is associated with thermo-oxidative degradation phenomena, where the breakage of bonds in the main chain and in the cross-linking networks occurs, as well as the formation of new cross-links of lower stability. South et al. (2003) demonstrated that the proportion of polysulfide bonds, which provide higher mechanical strength, progressively decreases with thermal aging, being replaced by mono- and disulfide bonds, which significantly deteriorates the material properties [19,21,34,35]. These findings are critical for the design of thermally cycled devices, such as seismic isolators, where mechanical integrity and energy dissipation capacity must be preserved over time.

3.1.3. Cyclic Shear (CS)

As shown in Figure 8, exposure to low temperatures increased the initial stiffness of both materials. The shear modulus of the UR-FREI increased by up to 63% with respect to the control specimens, while, in the UN-FREI, the increase was more moderate, in the order of 15%. This behavior can be attributed to the loss of mobility of the polymeric chains and to cold-induced crystallization processes, which tend to increase the stiffness of the material [22]. The variability in shear modulus was more pronounced, especially for UR-FREI specimens, due to the agglomerated structure of recycled rubber particles. We observed fluctuations of up to ±12% around the average shear modulus at high deformation levels (≥100% strain) in UR-FREI, compared to ±8% for UN-FREI.

Stiffening compromises the functionality of the isolators, since higher stiffness reduces the system's capacity to dampen earthquake-induced horizontal loads. In the case of UR-FREI, the specimens exposed to cold maintained a high shear modulus even with increasing

deformation, unlike the control specimen, which presented a progressive decrease. This indicates that cooling-induced stiffness inhibits the expected viscoelastic behavior and limits the energy dissipation capacity under cyclic loading. Such an effect can be explained by the segmental immobilization of the polymer chains and the development of stiff zones in the matrix, as has been reported in studies of the cryogenic behavior of elastomers [22,36]

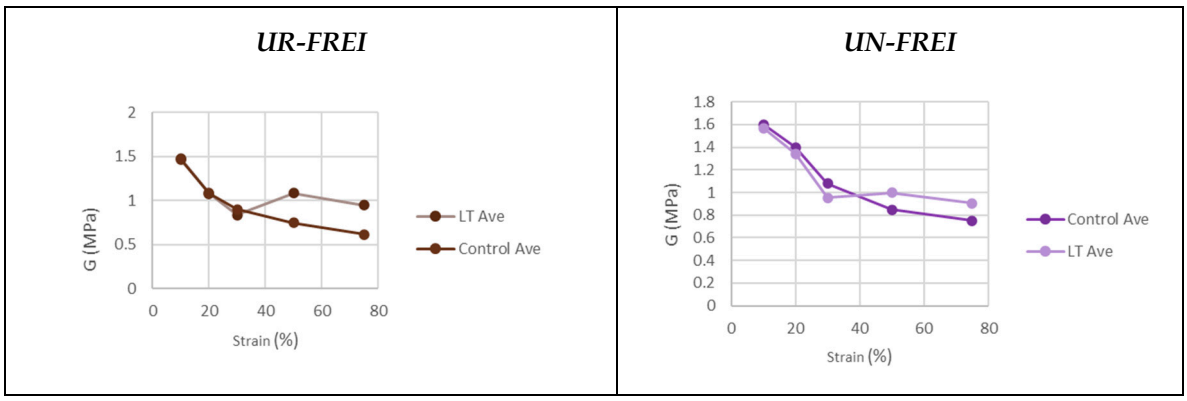


Figure 8. Cyclic shear results from exposure to low temperatures.

Figure 9 shows that accelerated thermal aging caused a significant increase in the stiffness of both matrices. Specifically, the shear modulus increased by 84% in UR-FREI and 64% in UN-FREI, compared to their respective reference samples. This increase in stiffness is attributed to the thermal oxidation-induced densification of the crosslinking network discussed previously [21].

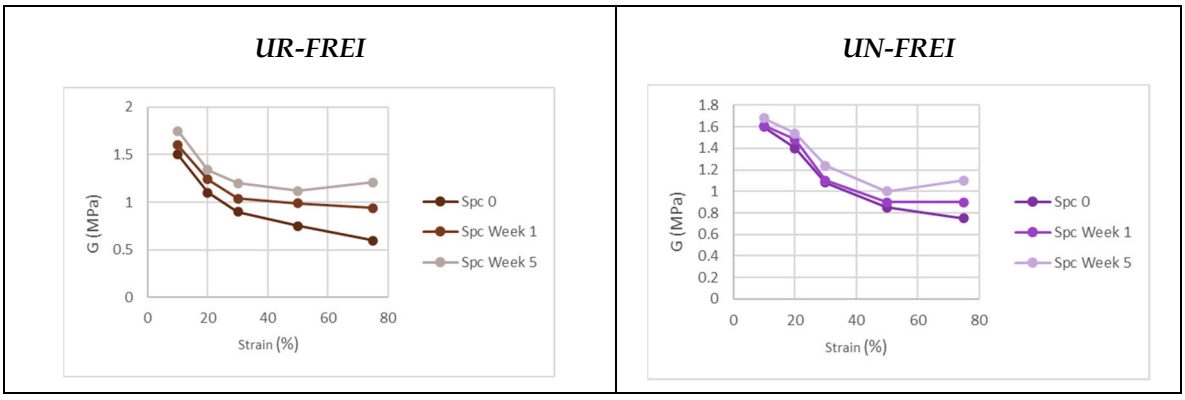


Figure 9. Cyclic shear results of accelerated aging.

These findings highlight the importance of considering thermal aging resistance in the selection of materials for seismic isolators. The loss of viscoelastic properties and reductions in energy dissipation capacity can compromise structural safety during seismic events.

3.1.4. Monotonic Compression (MC)

The results of the monotonic compression test (Figure 10) reveal a significant impact of low-temperature exposure on the mechanical behavior of both matrices evaluated. Under reference conditions (control specimens), both UR-FREI and UN-FREI showed typically nonlinear behavior, reaching 27.5 MPa and 60.2 MPa, respectively. However, when subjected to the cooling protocol, the matrices experienced a substantial decrease in their maximum load-carrying capacity under compression. In the case of UR-FREI, the strength was reduced by up to 58%, while, for UN-FREI, this reduction was close to 80%. This loss of strength is associated with the thermal embrittlement of the elastomers. The

literature reports that, as the temperature drops below the glass transition temperature, the polymer chains lose mobility, resulting in an increase in stiffness and a loss of toughness and deformation capacity [22,33].

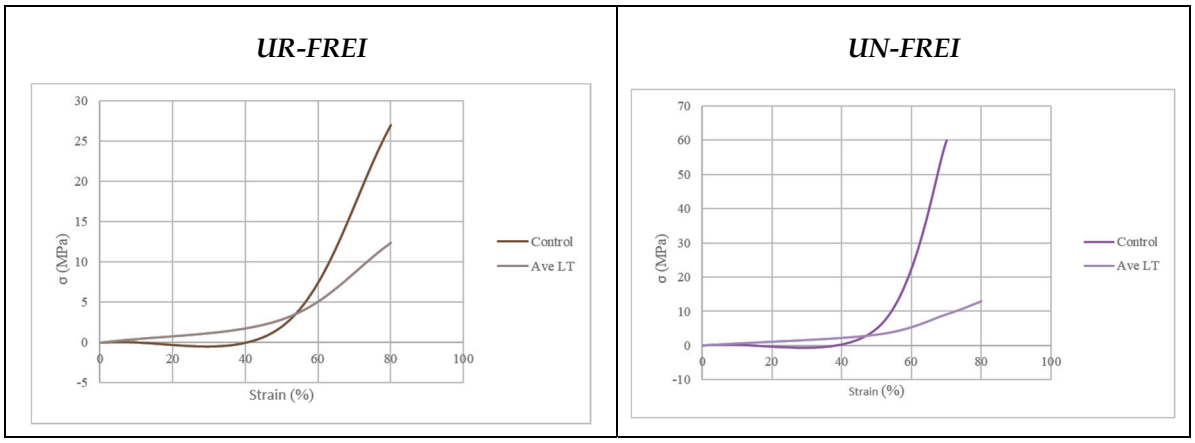


Figure 10. Monotonic compression test results at low temperatures.

The results of the monotonic compression tests showed a range of ±6% in maximum compressive stress for the UN-FREI specimens under control conditions, and a range of up to ±10% for the UR-FREI specimens. The response observed in UR-FREI suggests a lower monotonic compressive strength, possibly due to its agglomerated structure and the presence of interparticle voids, which act as internal stress concentrators during loading. This not only reduces the bearing capacity but also increases the risk of premature failure.

The results of the monotonic compression test, presented in Figure 11, show a progressive degradation of the mechanical capacity of both matrices as the time of exposure to thermal aging at 100 °C increases. The curves show a sustained decrease in the maximum stress reached by the specimens, accompanied by an evident loss of structural stiffness.

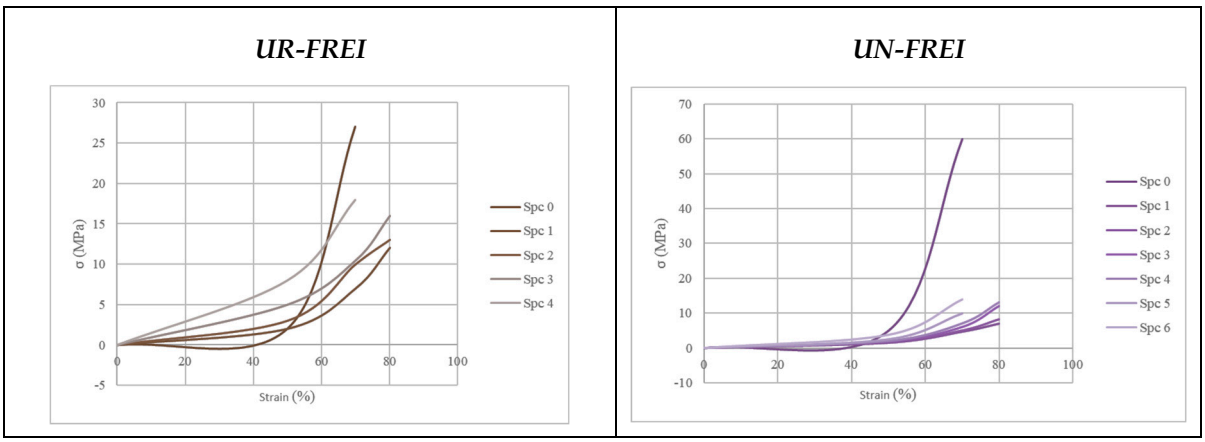


Figure 11. Monotonic compression test results under accelerated aging.

In the UR-FREI matrix, a 22% reduction in load capacity was observed with respect to the control specimen. From week 5 onwards, the specimens lost their original shape after the test and failed to recover, as shown in Illustration 14a. This permanent plastic deformation prevented the completion of the test for these samples, which is evidence of a functional collapse of the material. This behavior can be attributed to the degradation of the binder and the increase in porosity in the internal structure, factors that weaken the integrity of the composite against compressive loads. However, the UN-FREI matrix

showed a greater loss of strength than UR-FREI, close to 75%. Although the specimens retained their shape after the test, they showed surface fractures (Figure 12 and an elastic recovery of less than 12%. These effects are consistent with those reported in the literature for thermally aged elastomers, where oxidation promotes the breaking of bonds between polymer chains and the formation of stiffer but less resistant cross-linked networks, causing simultaneous decreases in elasticity and load-bearing capacity [21].

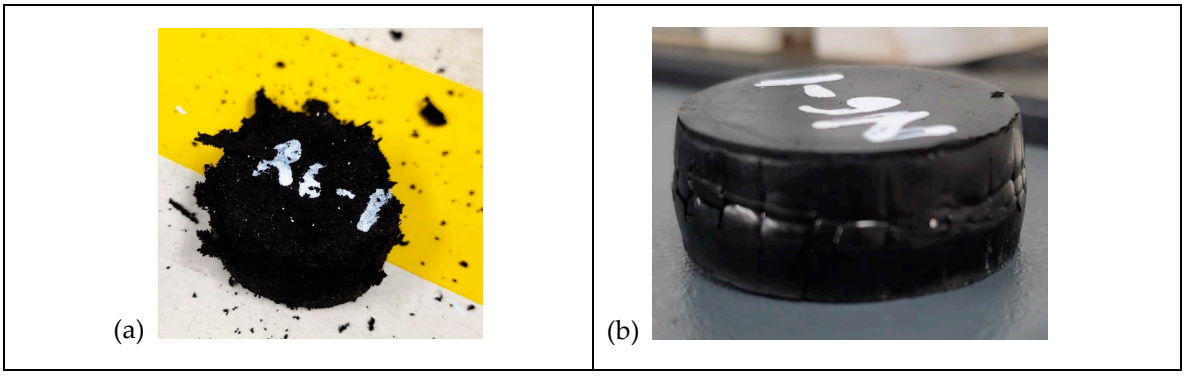


Figure 12. Monotonic compression test specimens. (**a**) UR-FREI (**b**) UN-FREI.

Table 2 summarizes the behavior of the UR-FREI and UN-FREI matrices against low temperatures and accelerated temperature aging in the different mechanical tests performed. It is observed that both factors affect the deformation capacity, strength, and stiffness of the matrices. In particular, thermal aging generated the most severe losses, especially in compression and tension. Although both matrices increase their toughness with cold, UR-FREI shows higher structural brittleness. These results show that, although both materials lose performance under extreme conditions, the UN-FREI matrix maintains better mechanical stability. This information is key for the selection of materials in seismic isolators, where the ability to withstand cyclic loads, dissipate energy and maintain structural integrity is critical for safety.

Table 2. Evaluation of the test results of UN-FREI and UR-FREI specimens.

	UR-FREI				UN-FREI			
Exposure	**H (Shore A)**	**T (σ)**	**CS (G)**	**MC (σ)**	**H (Shore A)**	**T (σ)**	**CS (G)**	**MC (σ)**
Low Temperatures	↑ 10%	↓ 76%	↑ 63%	↓ 58%	↑ 16%	↓ 21%	↑ 15%	↓ 80%
Accelerated Aging	↑ 15%	↓ 45%	↑ 84%	↓ 22%	↑ 25%	↓ 65%	↑ 64%	↓ 75%

3.2. Mechanical Evaluation of Prototypes Under Low-Temperature (LT) Conditions

3.2.1. Shear Compression Test

During the simultaneous shear and compression test, the horizontal stiffness (Kh) and effective damping (β) of the UR-FREI and UN-FREI prototypes subjected to low temperatures were evaluated. In the case of UR-FREI (Figure 13), a 57% decrease in horizontal stiffness and 19% decrease in damping was observed. This loss in damping capacity is consistent with the observed stiffening in the matrix, since the reduction in segmental mobility under low-temperature conditions limits energy dissipation. However, the drop in prototype stiffness seems to contradict the increase in shear modulus observed in the matrix. This apparent contradiction may be explained by the agglomerated internal structure of UR-FREI, consisting of recycled rubber particles and interstitial voids bound by a binder; at low temperatures, this configuration becomes more susceptible to the loss

of overall mechanical integrity, as the binder may crystallize or fail, affecting effective stress transfer.

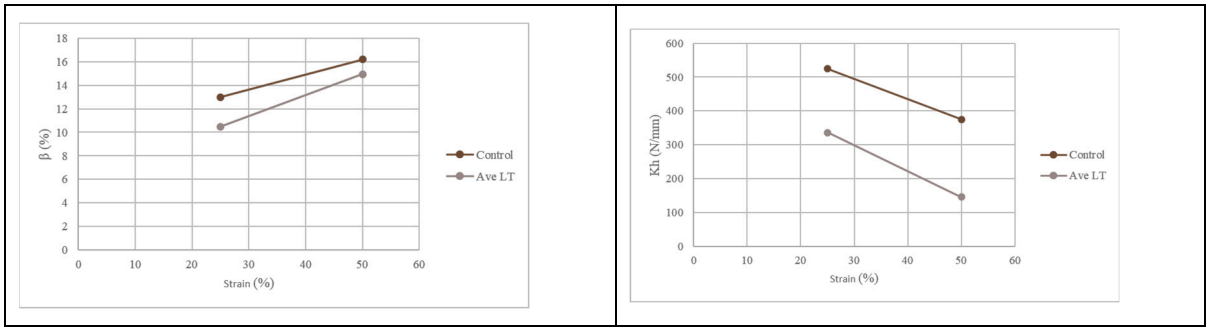


Figure 13. Damping and horizontal stiffness results of the UR-FREI prototypes exposed to low temperatures.

In contrast, the UN-FREI prototypes (Figure 14) showed a response consistent with their matrix: an 18% reduction in damping and a 25% increase in horizontal stiffness, reflecting structural stiffening without the loss of internal cohesion. These results reinforce the importance of considering not only the behavior of the matrix, but also the internal architecture of the material when evaluating its structural performance at the prototype scale.

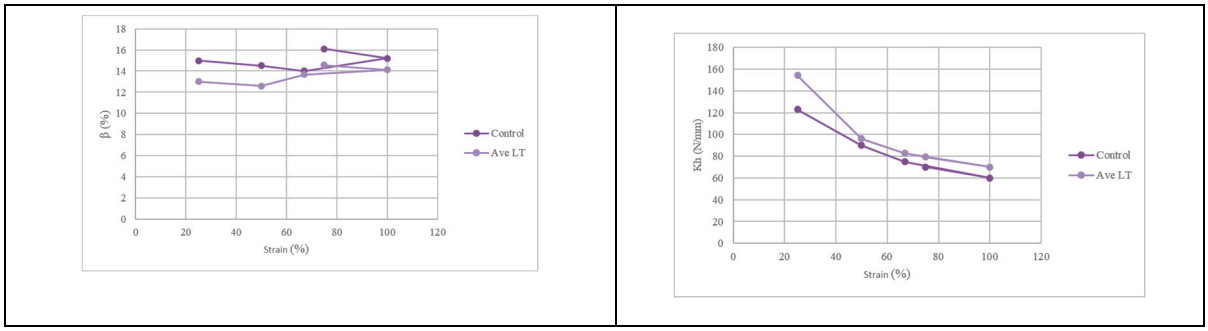


Figure 14. Damping and horizontal stiffness results of UN-FREI prototypes exposed to low temperatures.

3.2.2. Cyclic Compression Test

The vertical stiffness evaluation using the cyclic compression test allowed us to determine the effect of low temperatures on the ability of the insulator prototypes to withstand gravity loads under repeated stresses. As shown in Figure 15, both materials experienced a significant loss of stiffness: 28% in the UR-FREI and 44% in the UN-FREI prototypes, compared to their respective controls.

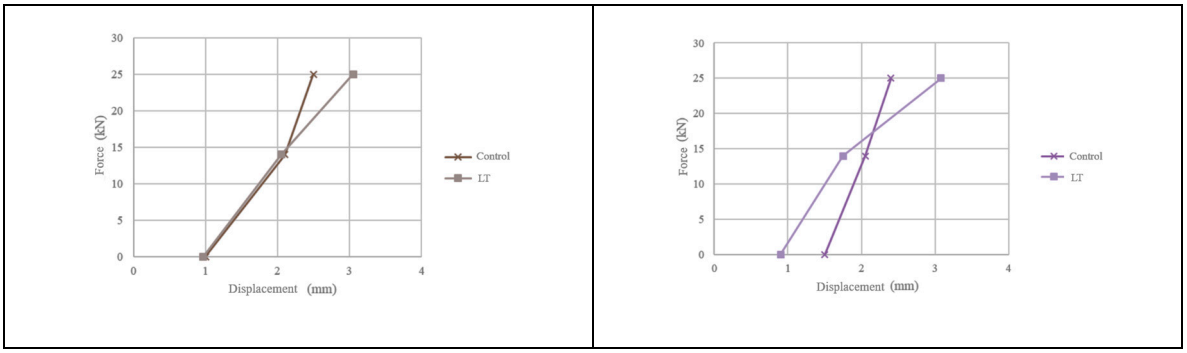


Figure 15. Vertical stiffness results at low temperatures.

In the case of UR-FREI, the loss of vertical stiffness is associated with the weakening of the internal structure under repeated loading, an effect amplified by the low cohesion of the bonded system under low-temperature conditions. Despite the higher local strength of the matrix, the prototype shows a functional reduction due to the accumulation of deformations and the progressive deterioration of the internal bonds, which limits its elastic recovery capacity after compression cycles. For UN-FREI, the greatest reduction in vertical stiffness can be attributed to the hardening of the natural rubber at low temperatures, which limits the mobility of the polymeric chains and reduces the material's ability to redistribute stresses and recover its original shape. Although this type of matrix retained its structural integrity better under shear and lateral deformations, it showed greater sensitivity to cyclic axial loads.

The following table (Table 3) shows a summary of the effect of low temperatures on the UR-FREI and UN-FREI isolator prototypes. A decrease in the mechanical performance of both systems is evidenced, especially in UR-FREI, due to its particulate nature. Considering their application as seismic isolators, it is essential to consider these functional losses, since they may compromise the system's capacity to dissipate energy and maintain structural stability under low-temperature conditions.

Table 3. Evaluation of the test results of UN-FREI and UR-FREI small-scale prototypes under LT conditions.

	UR-FREI			UN-FREI		
Exposure	**β (%)**	**Kh (N/mm)**	**Kv (kN)**	**β (%)**	**Kh (N/mm)**	**Kv (kN)**
Low Temperatures	↓ 19%	↓ 57%	↓ 28%	↓ 18%	↑ 25%	↓ 44%

3.3. Mechanical Evaluation of Prototypes with Accelerated Aging

3.3.1. Shear Compression Test

The results of the simultaneous shear and compression test allowed us to evaluate the impact of thermal aging on the damping (β) and horizontal stiffness (Kh) properties of the UR-FREI and UN-FREI prototypes. For UR-FREI, data are presented up to week 4 of curing (Figure 16), since, after this exposure time, the prototypes showed critical structural failures: loss of the external coating, exposure of reinforcement layers and slippage between interfaces, which prevented the continuation of the loading protocol.

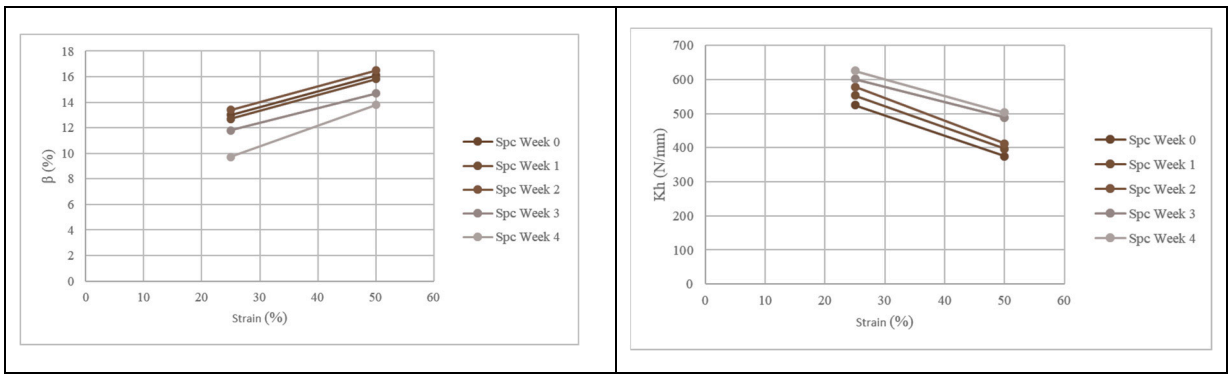


Figure 16. Results for damping and horizontal stiffness (accelerated aging of UR-FREI).

During the first few weeks, the UR-FREI devices exhibited a 13% decrease in damping and a 35% increase in horizontal stiffness: behavior consistent with the progressive hardening and stiffening of the matrix discussed in the previous tests (Section 3.1.1—Hardness

(H)). Thermal oxidation redistributes the density and type of crosslinking bonds, which raises the stiffness of the composite but reduces the ability of the system to dissipate energy.

In the UN-FREI prototypes (Figure 17), the effect of aging was more evident. A cumulative reduction of 53% in damping and an increase of up to 416% in horizontal stiffness was recorded after six weeks of curing. These results are in agreement with those reported by Russo and Cassiati, who attribute these effects to the oxidation of natural rubber, which causes a loss of elasticity, increased stiffness, and the degradation of viscoelastic behavior.

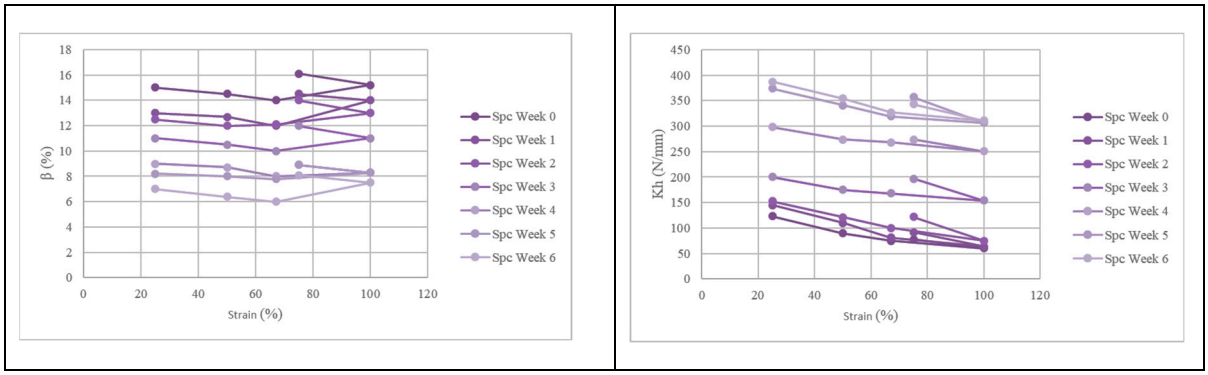


Figure 17. Results of damping and horizontal stiffness for the accelerated aging of UN-FREI.

The findings confirm that thermal aging critically affects the functional performance of isolators, especially their damping capacity. This should be considered in the design and validation of devices, particularly if they are intended to be used in harsh environmental conditions or for long durations.

3.3.2. Cyclic Compression Test

This test evaluated the effect of thermal aging on the vertical stiffness of the UR-FREI and UN-FREI prototypes. It is important to note that, due to the advanced degradation of the devices at week 6, they could not be tested: the outer coating presented a significant loss of structural integrity after prolonged exposure to 100 °C temperatures, preventing adequate load transfer during the test.

As shown in Figure 18, both UR-FREI and UN-FREI show a progressive decrease in vertical stiffness over time. The loss reaches 29% in the UR-FREI and 34% in the UN-FREI, values that show a significant effect on the bearing capacity of the devices. This behavior is consistent with the results obtained in the mechanical characterization of the aged matrices, where a substantial reduction in deformation capacity and tensile strength was observed.

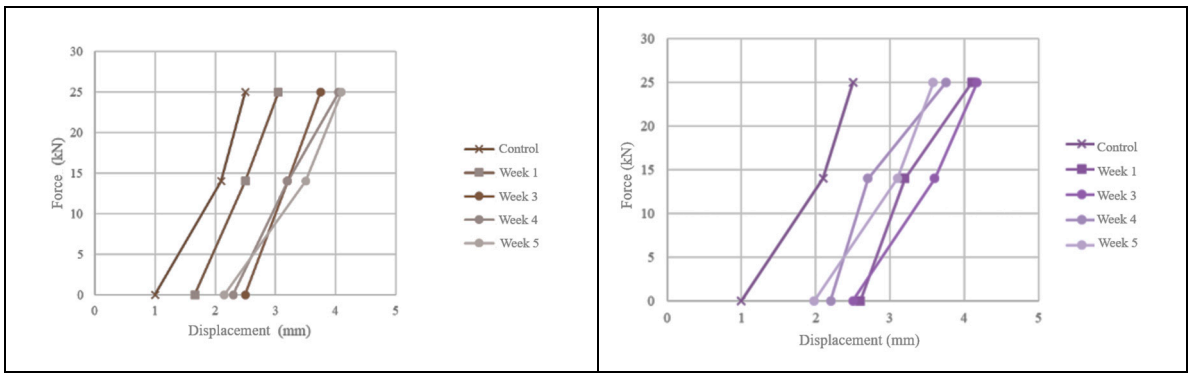


Figure 18. Results for vertical stiffness under the conditions of accelerated aging.

Although aging generates an initial increase in rubber stiffness at the microstructural level, this translates into brittleness at the macroscopic level. The formation of additional crosslinks, combined with oxidation processes and internal microcracking, decreases the material's capacity to absorb energy and recover its original shape under repeated loads. This loss of elastic behavior compromises the functionality of the insulator against vertical stresses, a critical aspect of its structural performance. Consequently, the results reinforce the need to consider the thermal stability of the constituent materials in the design of seismic isolators, especially if they are intended for environments with prolonged exposure to high temperatures.

Table 4 presents a summary of the effects of thermal aging on key properties of the UR-FREI and UN-FREI isolator prototypes. A general decrease in the damping and vertical stiffness of both systems is observed, which compromises their ability to dissipate energy and withstand gravity loads. However, UN-FREI experiences a pronounced increase in horizontal stiffness, associated with oxidation and densification processes of the monolithic matrix. In contrast, UR-FREI, although also increasing its lateral stiffness, shows less variation, probably because it is limited by the structural instability of its agglomerated configuration.

Table 4. Evaluation of the test results of UN-FREI and UR-FREI small-scale prototypes: aging.

	UR-FREI			UN-FREI		
Exposure	**β (%)**	**Kh (N/mm)**	**Kv (kN)**	**β (%)**	**Kh (N/mm)**	**Kv (kN)**
Accelerated Aging Test	↓ 13%	↑ 35%	↓ 29%	↓ 53%	↑ 416%	↓ 34%

3.4. Considerations for Improving the Design of Matrices and Devices

To improve the performance of seismic isolators under adverse conditions, several material and structural strategies may be considered. First, incorporating thermally stable elastomeric compounds such as ethylene propylene diene monomer (EPDM) rubber offers enhanced resistance to thermal oxidation and preserves mechanical integrity in low-temperature environments [37]. For matrices incorporating recycled rubber, the addition of compatibilizers such as ethylene-vinyl acetate (EVA) has been shown to improve interfacial adhesion between rubber particles, thereby mitigating early mechanical failure due to delamination or void propagation [38–40]. Structurally, the performance of the multilayer configuration can be improved by incorporating suitable fiber–matrix coupling agents. These agents enhance interfacial adhesion, strengthen cohesion between layers, and reduce the risk of delamination under cyclic thermal and mechanical loads [41].

4. Conclusions

- This study investigated the durability and mechanical performance of low-cost seismic isolators (UR-FREI and UN-FREI) under the combined effects of low temperatures and accelerated thermal aging. By conducting a systematic evaluation of both recycled and natural rubber matrices, as well as small-scale prototypes, this work aimed to address critical knowledge gaps in the long-term behavior of these alternative isolators. The results provide essential insights for their safe and reliable application in seismic risk mitigation, particularly in developing regions or environments characterized by significant thermal variation.
- The decreases in deformation capacity and maximum stress, together with the increase in shear modulus, show the critical behavior of the matrices under extreme thermal conditions. These changes increase the stiffness of the devices, but at the cost of a loss of flexibility, which compromises their ability to dissipate seismic energy.

- Low temperatures significantly affect the performance of unmodified natural rubber and agglomerated recycled rubber compounds. These materials tend to lose flexibility, exhibit reduced deformation capacity, and become brittle, which compromises their energy dissipation function. Therefore, their use is not recommended in cold regions, especially where high damping performance is required in seismic isolation applications.
- The results suggest the need to implement periodic evaluations of in-service devices. Visual inspections are recommended every five years to identify possible cracks in the coating, which could be indicative of progressive internal damage due to aging or environmental exposure.
- The current configuration of the arrays and the multilayer structure of the devices could lead to limitations in the efficient transfer of vertical and horizontal loads. This may result in the poor structural performance of the system and an increased risk of damage to both structural and non-structural elements during a seismic event.
- Based on the observed mechanical degradation under cold and thermally accelerated aging conditions, we recommend exploring design modifications in both the material formulation and multilayer architecture. The use of thermally stable elastomers, the incorporation of compatibilizers in recycled rubber matrices, and the application of fiber–matrix coupling agents in multilayer assemblies can significantly enhance the durability, cohesion, and overall seismic performance of isolation devices in demanding environments.

Author Contributions: Conceptualization, I.C.V.-C., E.D.L.-M., I.E.M.-S., M.A.R.-M., M.F.M.-V., O.C., S.J.D. and M.V.-L.; methodology, E.D.L.-M., I.C.V.-C., I.E.M.-S., M.A.R.-M., O.C., E.P., M.S.-B., S.J.D. and M.V.-L.; validation, I.C.V.-C., E.D.L.-M., I.E.M.-S., M.A.R.-M., O.C. and M.F.M.-V.; formal analysis, I.C.V.-C., E.D.L.-M., I.E.M.-S., M.A.R.-M., M.F.M.-V., O.C., S.J.D. and M.V.-L.; investigation, I.C.V.-C., E.D.L.-M., E.P., and M.S.-B.; resources, I.E.M.-S., M.A.R.-M., E.P., M.S.-B. and M.F.M.-V.; data curation, I.C.V.-C. and E.D.L.-M.; writing—original draft, I.C.V.-C., E.D.L.-M., I.E.M.-S., M.A.R.-M., M.F.M.-V., E.P., M.S.-B., S.J.D. and M.V.-L.; writing—review and editing, I.C.V.-C., E.D.L.-M., I.E.M.-S., M.A.R.-M., M.F.M.-V., O.C., E.P., M.S.-B., S.J.D. and M.V.-L.; visualization, I.C.V.-C., E.D.L.-M., I.E.M.-S., M.A.R.-M., M.F.M.-V., O.C., E.P., M.S.-B., S.J.D. and M.V.-L.; supervision, I.C.V.-C., I.E.M.-S., M.A.R.-M., M.F.M.-V., O.C., S.J.D. and M.V.-L.; project administration, I.E.M.-S. and M.A.R.-M.; funding acquisition, I.E.M.-S., M.A.R.-M. and O.C. All authors have read and agreed to the published version of the manuscript.

Funding: This research was funded by the program "852-2019 CONVOCATORIA DE PROGRAMAS CONECTANDO CONOCIMIENTO 2019—MINCIENCIAS". The entity that financed the project did not participate in the decision-making process related to the experiments or to the publication process of this article.

Data Availability Statement: The original contributions presented in this study are included in the article. Further inquiries can be directed to the corresponding author.

Acknowledgments: The authors acknowledge the Fulbright Colombia Scholar Program, as well as the distinguished professors and students at Purdue University, Universidad del Valle and Pontificia Universidad Javeriana in Cali especially the EPSILON, MATCON and SEEDE groups, for their valuable support during the experimental phase of this study. We would also like to thank the companies Surtidor Industrial S.A.S. and Occidental de Cauchos S.A.S. for their valuable support of this research. Finally, special acknowledgments are due to the program "852-2019 CONVOCATORIA DE PROGRAMAS CONECTANDO CONOCIMIENTO 2019—MINCIENCIAS".

Conflicts of Interest: The authors declare no conflicts of interest.

References

1. Naeim, F.; Kelly, J.M. *Design of Seismic Isolated Structures*; John Wiley & Sons, Inc.: Hoboken, NJ, USA, 1999. [CrossRef]
2. Kelly, J.M. Analysis of Fiber-Reinforced Elastomeric Isolators. *J. Seismol. Earthq. Eng.* **1992**, *1*, 19–34.
3. Taylor, A.W.; Lin, A.N.; Martin, J.W. Performance of Elastomers in Isolation Bearings: A Literature Review. *Earthq. Spectra* **1992**, *8*, 279–303. [CrossRef]
4. Furinghetti, M.; Pavese, A. Definition of a Simplified Design Procedure of Seismic Isolation Systems for Bridges. *Struct. Eng. Int.* **2020**, *30*, 381–386. [CrossRef]
5. Restrepo, M.G.; Madera Sierra, I.E.; Castellanos-Toro, S.; Marulanda, J. Impact of the Implementation of Unbonded Seismic Isolators on the Design and Retrofitting of Bridges. *Struct. Eng. Int.* **2023**, *33*, 677–688. [CrossRef]
6. Madera Sierra, I.E.; Marulanda Casas, J.; Thomson, P. Matrix and reinforcement materials for low-cost building isolators: An overview of results from experimental tests and numerical simulations. *J. Appl. Res. Technol.* **2018**, *17*, 44–56. [CrossRef]
7. Madera Sierra, I.E.; Losanno, D.; Strano, S.; Marulanda, J.; Thomson, P. Development and experimental behavior of HDR seismic isolators for low-rise residential buildings. *Eng. Struct.* **2019**, *183*, 894–906. [CrossRef]
8. *AASHTO M251-06*; Standard Specification for Plain and Laminated Elastomeric Bridge Bearings. American Association of State Highway and Transportation Officials: Washington, DC, USA, 2016. Available online: https://www.arpminc.com/publications/44 (accessed on 5 May 2025).
9. Madera-Sierra, I.E. Desarrollo Tecnológico de un Aislador Sísmico de Bajo Costo para Edificaciones Bajas. Ph.D. Thesis, Universidad del Valle, Cali, Colombia, 2018.
10. Ortega, L. Prototipos de Aisladores Sísmicos con Matriz de Caucho Reciclado para la Mitigación de Riesgo en Estructuras. Master's Thesis, Universidad del Valle, Cali, Colombia, 2022.
11. Losanno, D.; De Domenico, D.; Madera-Sierra, I.E. Experimental testing of full-scale fiber reinforced elastomeric isolators (FREIs) in unbounded configuration. *Eng. Struct.* **2022**, *260*, 114234. [CrossRef]
12. Losanno, D.; Serino, G.; Marulanda, J.; Spizzuoco, M.; Madera-Sierra, I.E.; Thomson, P.; Calabrese, A. Recycled versus Natural-Rubber Fiber-Reinforced Bearings for Base Isolation: Review of the Experimental Findings. *J. Earthq. Eng.* **2020**, *26*, 1921–1940. [CrossRef]
13. Losanno, D.; Madera Sierra, I.E.; Spizzuoco, M.; Marulanda, J.; Thomson, P. Experimental performance of unbonded polyester and carbon fiber reinforced elastomeric isolators under bidirectional seismic excitation. *Eng. Struct.* **2020**, *209*, 110003. [CrossRef]
14. Losanno, D.; Madera Sierra, I.E.; Spizzuoco, M.; Marulanda, J.; Thomson, P. Experimental assessment and analytical modeling of novel fiber-reinforced isolators in unbounded configuration. *Compos. Struct.* **2019**, *212*, 66–82. [CrossRef]
15. Rodriguez-Piedrahita, J.S.; Muñoz-Gutierrez, L.A.; Madera-Sierra, I.E.; Pérez-Ruiz, D.D.; Cundumí-Sanchez, O. Hyperelastic and Viscoelastic Properties of Recycled Rubber Material—Experimental and Fem Characterization Study. *Polym. Test.* **2025**, *149*, 108870. [CrossRef]
16. Meza-Muñoz, A.O.; Dyke, S.J.; Rojas-Manzano, M.A.; Madera-Sierra, I.E.; Patino-Reyes, E.D.; Salmerón-Becerra, M.I.; Rivas-Ordoñez, F.S. Development of a Matrix for Seismic Isolators Using Recycled Rubber from Vehicle Tires. *Polymers* **2024**, *16*, 2977. [CrossRef] [PubMed]
17. Rivas-Ordonez, F.S.; Dyke, S.J.; Meza-Munoz, A.O.; Madera-Sierra, I.E.; Rojas-Manzano, M.A.; Patino, E.D.; Salmerón-Becerra, M.I. Alternatives for Enhancing Mechanical Properties of Recycled Rubber Seismic Isolators. *Polymers* **2024**, *16*, 2258. [CrossRef]
18. Lemos-Micolta, E.D.; Dyke, S.J.; Velay-Lizancos, M.; Rojas-Manzano, M.A.; Cundumí, O.; Velasco-Cuervo, I.C.; Madera-Sierra, I.E.; Patino, E.; Salmeron-Becerra, M.; Lopez-Arias, M. Assessment of the Mechanical Properties of Low-Cost Seismic Isolators Exposed to Environmental Conditions. *Appl. Sci.* **2025**, *15*, 346. [CrossRef]
19. Calabrese, A.; Losanno, D.; Barjani, A.; Spizzuoco, M.; Strano, S. Effects of the long-term aging of glass-fiber reinforced bearings (FRBs) on the seismic response of a base-isolated residential building. *Eng. Struct.* **2020**, *221*, 110735. [CrossRef]
20. Toopchi-Nezhad, H.; Ghotb, M.R.; Al-Anany, Y.M.; Tait, M.J. Partially bonded fiber reinforced elastomeric bearings: Feasibility, effectiveness, aging effects, and low temperature response. *Eng. Struct.* **2019**, *179*, 120–128. [CrossRef]
21. South, J.T.; Case, S.W.; Reifsnider, K.L. Effects of Thermal Aging on The Mechanical Properties of Natural Rubber. *Rubber Chem. Technol.* **2003**, *76*, 785–802. [CrossRef]
22. Yu, L.; Liu, S.; Yang, W.; Liu, M. Analysis of Mechanical Properties and Mechanism of Natural Rubber Waterstop after Aging in Low-Temperature Environment. *Polymers* **2021**, *13*, 2119. [CrossRef]
23. Losanno, D.; Spizzuoco, M.; Calabrese, A. Bidirectional shaking-table tests of unbonded recycled-rubber fiber-reinforced bearings (RR-FRBs). *Struct. Control Health Monit.* **2019**, *26*, e2386. [CrossRef]
24. *ASTM D746*; Test Method for Brittleness Temperature of Plastics and Elastomers by Impact. ASTM International: West Conshohocken, PA, USA, 2020. [CrossRef]
25. *ASTM D2240*; Test Method for Rubber Property—Durometer Hardness. ASTM International: West Conshohocken, PA, USA, 2015. [CrossRef]

26. *ASTM D0412*; Test Methods for Vulcanized Rubber and Thermoplastic Elastomers—Tension. ASTM International: West Conshohocken, PA, USA, 2006. [CrossRef]
27. *ASTM D4014*; Standard Specification for Plain and Steel-Laminated Elastomeric Bearings for Bridges. ASTM International: West Conshohocken, PA, USA, 2018.
28. *ASTM D575*; Test Methods for Rubber Properties in Compression. ASTM International: West Conshohocken, PA, USA, 2018. [CrossRef]
29. Kunal, K.; Robertson, C.G.; Pawlus, S.; Hahn, S.F.; Sokolov, A.P. Role of Chemical Structure in Fragility of Polymers: A Qualitative Picture. *Macromolecules* **2008**, *41*, 7232–7238. [CrossRef]
30. Properties of Rubber at Low Temperatures. *Nature* **1942**, *149*, 645. [CrossRef]
31. Fuller, K.N.G.; Gough, J.; Thomas, A.G. The effect of low-temperature crystallization on the mechanical behavior of rubber. *J. Polym. Sci. B Polym. Phys.* **2004**, *42*, 2181–2190. [CrossRef]
32. Cossio Urán, E.; Giraldo Vásquez, D.; Castaño, N. Efectos del envejecimiento térmico y del contenido de negro de humo en la resistencia al desgaste abrasivo en seco del caucho natural. *El Hombre Y La Máquina* **2011**, *36*, 115–122.
33. Kabakçi, G.C.; Aslan, O.; Bayraktar, E. A Review on Analysis of Reinforced Recycled Rubber Composites. *J. Compos. Sci.* **2022**, *6*, 225. [CrossRef]
34. Hamaguchi, H.; Aizawa, S.; Samejima, Y.; Kikuchi, T.; Suzuki, S.; Yoshizawa, T. A Study of Aging Effect on a Rubber Bearing After About Twenty Years in Use. *AIJ J. Technol. Des.* **2009**, *15*, 393–398. [CrossRef]
35. Wright, K.R.S.; Botha, T.R.; Els, P.S. Effects of age and wear on the stiffness and friction properties of an SUV tyre. *J. Terramech.* **2019**, *84*, 21–30. [CrossRef]
36. Menard, K. Analyzing Tire Rubbers in the DMA 8000. Available online: https://www.researchgate.net/publication/293525637 (accessed on 27 June 2024).
37. Zhu, X.; Li, X.; Jing, H.; Chen, Y.; Hou, L.; Bai, Y.; Jiang, Q.; Tang, C.; Chen, J. Rubber compounds made of modified ethylene propylene diene monomer (EPDM) for laminated bearings with excellent anti-peel strength. *Constr. Build. Mater.* **2024**, *443*, 137686. [CrossRef]
38. Liang, J.; Ngai, T.; Wang, C.; Sang, J.; Lin, W.; Ren, K.; Wu, J. Ethylene vinyl acetate as a multifunctional compatibilizer for natural rubber/cis-1,4-polybutadiene rubber blends with enhanced compatibility, filler dispersion and mechanical properties. *Collagen Leather* **2025**, *7*, 3. [CrossRef]
39. Ramarad, S.; Ratnam, C.T.; Munusamy, Y.; Rahim, N.A.A.; Muniyadi, M. Thermochemical compatibilization of reclaimed tire rubber/ poly(ethylene-co-vinyl acetate) blend using electron beam irradiation and amine-based chemical. *J. Polym. Res.* **2021**, *28*, 389. [CrossRef]
40. Fazli, A.; Rodrigue, D. Thermoplastic elastomers based on recycled high-density polyethylene/ground tire rubber/ethylene vinyl acetate: Effect of ground tire rubber regeneration on morphological and mechanical properties. *J. Thermoplast. Compos. Mater.* **2023**, *36*, 2285–2310. [CrossRef]
41. Meng, X.; Kang, L.; Guo, X.; Tang, X.; Liu, L.; Shen, M. Highly Strong Interface Adhesion of Polyester Fiber Rubber Composite via Fiber Surface Modification by Meta-Cresol/Formaldehyde Latex Dipping Emulsion. *Polymers* **2023**, *15*, 1009. [CrossRef] [PubMed]

Disclaimer/Publisher's Note: The statements, opinions and data contained in all publications are solely those of the individual author(s) and contributor(s) and not of MDPI and/or the editor(s). MDPI and/or the editor(s) disclaim responsibility for any injury to people or property resulting from any ideas, methods, instructions or products referred to in the content.